Perturbative NLO $\not\pi$EFT for future LQCD finite-volume results

(arXiv:2402.04817 [nucl-th] (2024), accepted in Phys. Rev. D)

Martin Schäfer

Nuclear Physics Institute, Czech Academy of Sciences, Řež, Czech Republic

Tafat Weiss-Attia, Betzalel Bazak

The Racah Institute of Physics, Hebrew University of Jerusalem

ECT* workshop SPICE: Strange hadrons as a Precision tool for strongly InteraCting systEms

Effective Field Theory (EFT)

- **Effective field theory** (EFT) enables to systematically describe physical phenomena at momenta Q,
  while the underlying theory is valid at a higher mass scale M_{hi}, $Q \ll M_{hi}$.
- The interactions are written in terms of **low energy degrees of freedom**, while retaining the symmetries of the underlying theory.
- The details of the short-range dynamics are encoded in the **interaction strengths** (low energy constants, LECs).

$\not\pi$EFT

- EFTs are used in nuclear physics to realize **QCD** in terms of **hadrons**, instead of quarks and gluons.
- In **$\not\pi$EFT**, nucleons are the sole degrees of freedom and the pion exchange is integrated out.

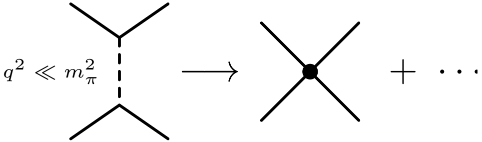

W. Hammer, S. König, and U. van Kolck, Rev. Mod. Phys. **92**, 025004 (2020).

$\not\pi$EFT power counting

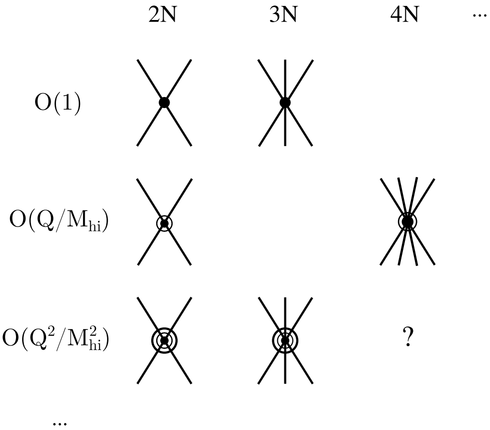

W. Hammer, S. König, and U. van Kolck, Rev. Mod. Phys. **92**, 025004 (2020).

$\not\pi$EFT at LO

- The leading-order (LO) potential:

$$\hat{V}_{LO} = \sum_{i<j} V_{S=1,T=0}(\boldsymbol{r}_{ij}) + V_{S=0,T=1}(\boldsymbol{r}_{ij}) + \sum_{i<j<k} V_3(\boldsymbol{r}_{ij}, \boldsymbol{r}_{jk})$$

$$V_{S,T}(\boldsymbol{r}_{ij}) = C^{(0)}_{S,T}(\Lambda)\hat{P}_{S,T} G_\Lambda(\boldsymbol{r}_{ij})$$

$$V_3(\boldsymbol{r}_{ij}, \boldsymbol{r}_{jk}) = D^{(0)}_1(\Lambda)\hat{P}_{1/2,1/2} G_\Lambda(\boldsymbol{r}_{ij}) G_\Lambda(\boldsymbol{r}_{jk})$$

- Regularization scheme:

$$G_\Lambda(r) = \frac{\Lambda^3}{8\pi^{3/2}} \exp[-\frac{\Lambda^2}{4}\boldsymbol{r}^2]$$

The leading order is **iterated**.

$\not\pi$EFT at NLO

- Next-to-leading order (NLO) potential:

$$
\begin{aligned}
V_{\mathrm{NLO}} = \tilde{V}_{\mathrm{LO}} + & \\
& + \sum_{i<j} \left(C^{(1)}_{0,1}(\Lambda)\hat{P}_{0,1} + C^{(1)}_{1,0}(\Lambda)\hat{P}_{1,0} \right) \cdot \\
& \cdot \left(G_\Lambda(\boldsymbol{r}_{ij})\overrightarrow{\nabla}^2_{ij} + \overleftarrow{\nabla}^2_{ij} G_\Lambda(\boldsymbol{r}_{ij}) \right)
\end{aligned}
$$

Renormalization problems due to the Wigner bound, the NLO terms are **treated perturbatively**.

$\not{\pi}$**EFT** in finite-volume

Periodicity:
Inside a box of size $L \times L \times L$ with periodic boundary conditions, the potential is periodicised,

$$V_L(\boldsymbol{r}_1, \boldsymbol{r}_2, \dots) = \sum_{\boldsymbol{n}_1, \boldsymbol{n}_2, \dots} V(\boldsymbol{r}_1 + L\boldsymbol{n}_1, \boldsymbol{r}_2 + L\boldsymbol{n}_2, \dots).$$

Therefore, the Gaussian regulator is modified,

$$G_{\Lambda,\mathrm{p.b.c}}(r) = \frac{\Lambda^3}{8\pi^{3/2}} \sum_{\boldsymbol{q} \in \mathbb{Z}^3} \exp[-\frac{\Lambda^2}{4}(\boldsymbol{r} - L\boldsymbol{q})^2]$$

SVM in free-space

- We solve numerically the N-body Schrödinger equation with the **stochastic variational method** (SVM).
- The wave function is expanded over a **correlated Gaussian basis**,

$$\Psi = \sum_i c_i \hat{\mathcal{A}} \left\{ G_i(A_i; \boldsymbol{r}) \chi_{SM_S} \xi_{IM_I} \right\}$$

- The correlated Gaussians are given by,

$$G_i(A_i; \boldsymbol{r}) = \exp\left[-\frac{1}{2} \boldsymbol{r}^T A_i \boldsymbol{r} \right]$$

$\boldsymbol{r}$ is a vector of all single-particle coordinates,

$$\boldsymbol{r} = (\boldsymbol{r}_1, \boldsymbol{r}_2, ..., \boldsymbol{r}_N)^T$$

SVM in free-space

- The **energy** and the **coefficients** c_i are obtained by solving the generalized eigenvalue problem,

$$\mathcal{H}\mathbf{c} = E\mathcal{N}\mathbf{c}$$

$$\mathcal{H}_{ij} = \langle G_i|H|G_j\rangle \qquad \mathcal{N}_{ij} = \langle G_i|G_j\rangle$$

- The **non-linear parameters** A_i are chosen stochastically to minimize the energy.

SVM in finite-volume

- In **box-SVM**, the wave-function is periodic in the box size,

$$\Psi_L(\boldsymbol{r}_1, \boldsymbol{r}_2, \dots) = \Psi_L(\boldsymbol{r}_1 + L\boldsymbol{n}_1, \boldsymbol{r}_2 + L\boldsymbol{n}_2, \dots).$$

- Periodicised Gaussian basis function:

$$G_L(A_i; \boldsymbol{r}) = \sum_{\boldsymbol{b} \in \mathbb{Z}^{3N}} \exp\left[-\frac{1}{2}\left(\boldsymbol{r} - L\boldsymbol{b}\right)^T A_i \left(\boldsymbol{r} - L\boldsymbol{b}\right)\right]$$

X. Yin and D. Blume, Phys. Rev. A **87**, 063609 (2013).

Extrapolation of LQCD results

- Finite-volume $\not\pi$EFT can be fitted using **LQCD results**.
- The EFT is then solved in free space to obtain **physical observables**.

M. Eliyahu, B. Bazak and N. Barnea, Phys. Rev. C **102**, 044003 (2020).

W. Detmold and P. E. Shanahan, Phys. Rev. D **103**, 074503 (2021).

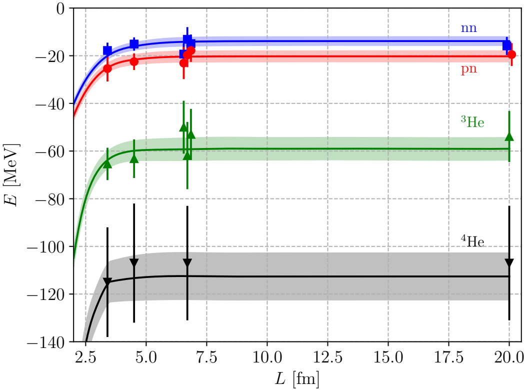

Symbols represent NPLQCD results for $m_\pi = 806$ MeV, from S.R. Beane *et al.*, Phys. Rev. D 87, 034506 (2013). Curves represent $\not\pi$EFT results obtained by M. Eliyahu *et al.*

Lüscher formalism

Scale separation - $R \ll \kappa^{-1} \ll L$
Lüscher two-body **bound state** formula:

$$B_2(L) = B_2^{\text{free}} + \frac{6\kappa_2|\mathcal{A}_2|^2}{\mu_2 L} e^{-\kappa_2 L} + \mathcal{O}(e^{-\sqrt{2}\kappa_2 L}), \quad \kappa_2 = \sqrt{2\mu_2 B_2^{\text{free}}}$$

M. Lüscher, Commun. Math. Phys. **104**, 177 (1986).

Generalization to an N-body bound state, S. König and D. Lee, Phys. Lett. B **779**, 9 (2018).

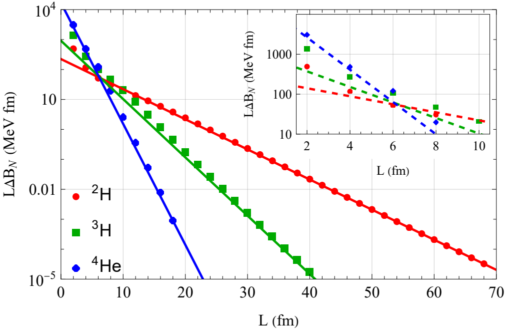

The energy shift ΔB_N due to the box, multiplied by the box size L, as function of L.

R. Yaron *et al.*,

Phys. Rev. D **106**

014511 (2022).

Lüscher formalism

Lüscher two-body **scattering state** formula:

$$k_L \cot\delta_0 = \frac{1}{\pi L} S\left[\left(\frac{Lk_L}{2\pi}\right)^2\right], \quad S(\eta) \equiv \lim_{\Omega\to\infty}\left(\sum_{\boldsymbol{j}\in\mathbb{Z}^3}^{\Omega} \frac{1}{|\boldsymbol{j}|^2-\eta} - 4\pi\Omega\right)$$

M. Lüscher, Commun. Math. Phys. **105**, 153 (1986); Nucl. Phys. B **354**, 531 (1991).

Effective range expansion:

$$k \cot\delta_0(k) = -\frac{1}{a_0} + \frac{1}{2} r_0 k^2 + \mathcal{O}(k^4)$$

Binding energy:

$$B_2 \approx \frac{1}{m a_0^2}\left(1 - \frac{r_0}{a_0}\right)^{-1}$$

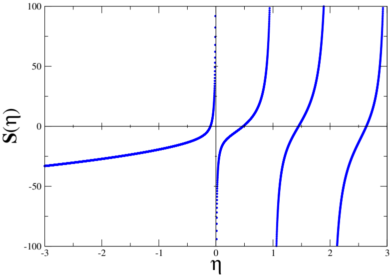

S. R. Beane *et al.*, Phys. Lett. B 585 (2004).

$\not\pi$EFT at NLO for nuclei in finite volume

W. Detmold *et al.*, **Constraint of pionless EFT using two-nucleon spectra from lattice QCD**. Phys. Rev. D **108**, 034509 (2023).

- Naive power counting at NLO.
- Non-perturbative inclusion of the NLO.

$\not\pi$EFT at NLO for nuclei in finite volume

- Fit finite-volume $\not\pi$EFT at NLO to finite-volume data, varying the box size.
- Solve the same EFT in free-space and calculate s-wave observables.
- Compare with the Lüscher formalism, fit to the same finite-volume data as the EFT was fitted to, and benchmark with known results.

Perturbative application of next-to-leading order pionless EFT for $A \leq 3$ nuclei in a finite volume.

Tafat Weiss-Attia, Martin Schäfer and Betzalel Bazak, arXiv:2402.04817 (2024) accepted in Phys. Rev. D.

Input data

The A_1^+ spectra of $A \leq 3$ nuclei in a box with periodic boundary conditions, interacting via the phenomenological NN Minnesota potential:

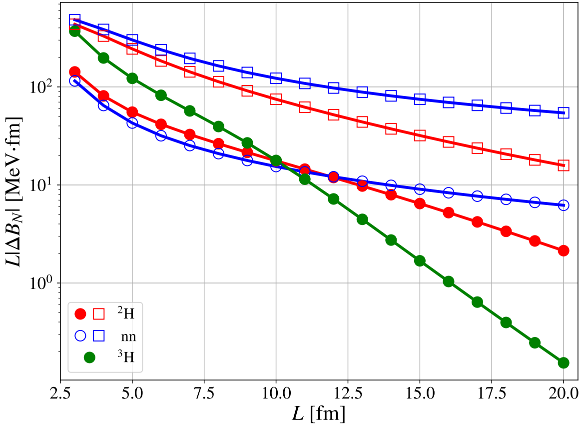

NN s-wave phase shifts with the Lüscher formalism

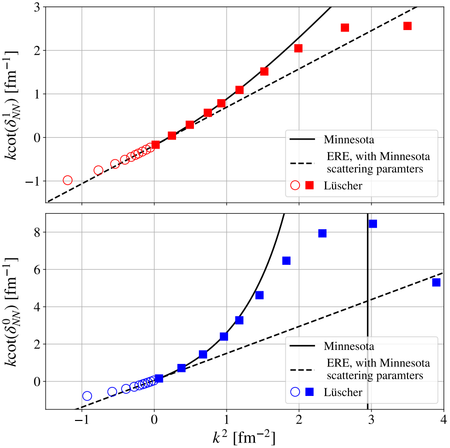

The NN s-wave phase shifts, presented as $k\cot(\delta_{NN})$, for the deuteron (upper panel) and dineutron (lower panel) channels plotted as a function k^2.

Deuteron binding energy

Upper panel - using ground and excited state energies from one box size L.

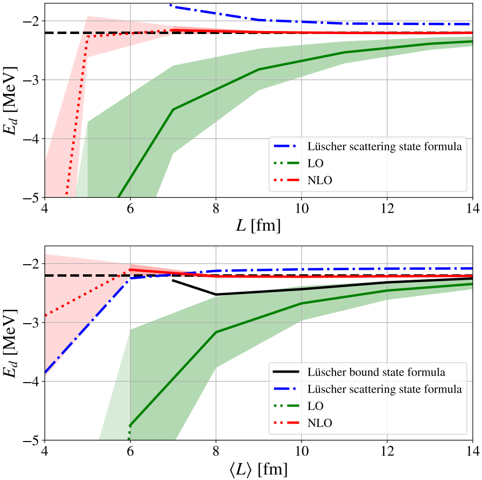

Lower panel - using ground state energies from two adjacent boxes, $\langle L \rangle \pm 1$.

The free-space deuteron binding energy E_d extracted from finite-volume energies, as function of the box size, L (upper panel), or average box, $\langle L \rangle$ (lower panel), used.

NN spin-triplet scattering length and effective range

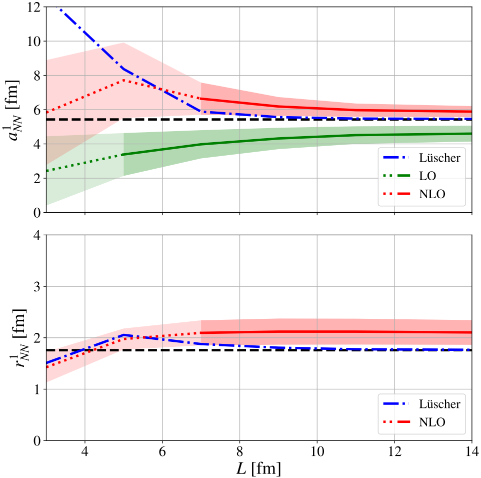

The free-space NN spin-triplet scattering length (upper panel) and effective range (lower panel) extracted from finite-volume energies, as function of the box size used.

NN spin-singlet scattering length and effective range

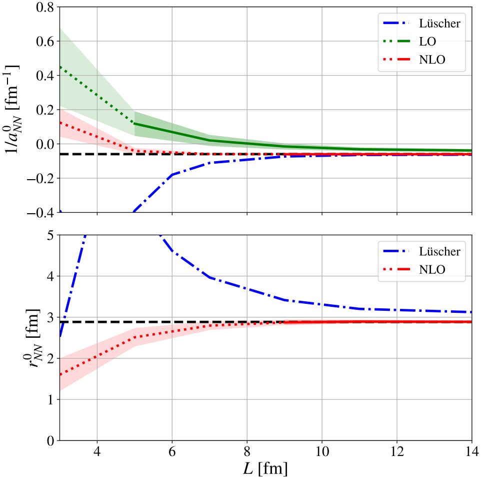

The free-space NN spin-singlet scattering length (upper panel) and effective range (lower panel) extracted from finite-volume energies, as function of the box size used.

Triton channel and nd spin-quartet scattering

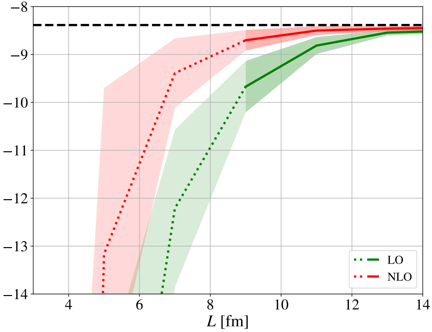

e free-space triton binding energy E_t extracted from
ite-volume energies, as function of the box size used.

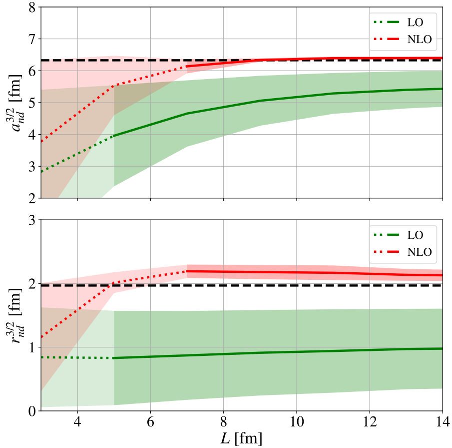

The free-space nd spin-quartet scattering length (upper panel) and effective range (lower panel) extracted from finite-volume energies, as function of the box size used.

Propagation of finite-volume data uncertainties

Propagation of uncertainties, assuming a 5% statistical uncertainty in the input data.

		$L=5$		$L=7$	
	Minnesota	Lüscher	NLO	Lüscher	NLO
E_d [MeV]	-2.2	-0.8(7)	-2.5(8)	-1.8(4)	-2.2(4)
a^1_{NN} [fm]	5.4	8.4(3.1)	6.1(8)	5.9(5)	6.3(6)
r^1_{NN} [fm]	1.7	2.1(3)	1.8(1)	1.9(2)	2.0(2)
$1/a^0_{NN}$[fm^{-1}]	-0.058	-0.4(3)	-0.02(2)	-0.11(5)	-0.05(2)
r^0_{NN}[fm]	2.885	5.8(3.2)	2.3(2)	4(1)	2.7(3)

a^1_{NN} with $L=5$ fm: Lüscher $\sim 37\%$, $\not\pi$EFT at NLO $\sim 13\%$.
r^0_{NN} with $L=7$ fm: Lüscher $\sim 26\%$, $\not\pi$EFT at NLO $\sim 10\%$.

Conclusions and summary

- $\not\pi$EFT up to NLO and the Lüscher formalism are employed to obtain **predictions** for free-space binding energies and s-wave scattering parameters of two- and three-nucleon systems, based on finite-volume spectrum.
- $\not\pi$EFT at NLO generally yields accurate predictions when box sizes of $L = 5, 7$ fm are used, whereas Lüscher predictions typically require larger box sizes of $L \geq 9$ fm.
- $\not\pi$EFT proves to be a powerful extrapolation tool, and allows the extraction of physical observations with a limited amount of input data.